Post-developmental extracellular proteoglycan maintenance in attractin-deficient mice

Abdallah Azouz
University of Tennessee Health Science Center College of Medicine Memphis
Jonathan Duke-Cohan (jonathan_duke-cohan@dfci.harvard.edu)
Dana-Farber Cancer Institute https://orcid.org/0000-0002-9478-9609

Research note

Keywords: Attractin, Extracellular matrix, Histology, Kidney, Liver, Proteoglycan

Posted Date: April 13th, 2020

DOI: https://doi.org/10.21203/rs.3.rs-20834/v1

Version of Record: A version of this preprint was published on June 24th, 2020. See the published version at https://doi.org/10.1186/s13104-020-05130-1.

Abstract

Objective: Neurodegeneration and hair pigmentation alterations in mice occur consequent to aberrations at the Atrn locus coding for the transmembrane form of attractin. Earlier results pointed to a possible involvement in intracellular trafficking/export of secretory vesicles containing proteoglycan. Here we examined kidney and liver, both heavily dependent upon proteoglycan, of attractin-deficient mice to determine whether abnormalities were observed in these tissues.

Results: Histological and histochemical analysis to detect glycosylated protein identified a severe loss in attractin-deficient mice of extracellular proteoglycan between kidney tubules in addition to a loss of glycosylated material within the intratubular brush border. In the liver, extracellular matrix material was significantly depleted between hepatocytes together with swollen sinuses and aberrations in the proteoglycan-dependent space of Disse. These results are consistent with a generalized defect in extracellular proteoglycan deposition in Atrn -mutant mice and support previous reports suggesting a role for attractin in the secretory vesicle pathway.

Introduction:

Attractin, initially discovered as a human secreted glycoprotein circulating at high concentrations in the periphery and enabling T cell-monocyte clustering (1), also exists as a transmembrane form produced by alternative splicing of the *ATRN* gene, while the mouse only produces the transmembrane form (2, 3). On activated T cells, attractin moves in electron-dense proteoglycan-rich vesicles to the plasma membrane leading to transient extracellular expression (1, 4). Mutations at the *Atrn* locus in the mouse result in the *mahogany* phenotype where, despite normal levels of the agouti protein that acts as an antagonist of α-melanocyte stimulating hormone (α-MSH), the agouti protein does not appear to be appropriately presented to the Melanocortin-1 receptor (Mc1R) and black/brown eumelanin synthesis persists rather than that of the lighter yellowish phaeomelanin (2). Attractin's role in agouti presentation remains to be fully elucidated. One possibility is that the membrane-anchored ectodomain may help present agouti protein by binding the positive N-terminal leaving the C-terminal free to interact with the Mc1R (5).

Attractin's functional range has widened following reports that *mahogany* ($Atrn^{mg-3J/mg-3J}$) mice present a juvenile-onset Central Nervous System (CNS)-confined neurodegeneration characterized by hypomyelination, axonal swelling, spongiform vacuolation and microtremors (5). This neural phenotype is found not only in other mouse mutant *Atrn* alleles (6, 7) but also in the *zitter* and *myelin vacuolation* rats (8, 9), and the *black tremor* hamster (10), all now confirmed as *Atrn* mutants. The pigmentation phenotype and neuropathology are corrected in animals transgenic for membrane attractin (5, 8). Embryonic development appears normal in *Atrn*-mutant mice; the neurodegeneration is manifest during juvenile maturation and may be related to a defect in maintaining the integrity of the plasma membrane with potentially severe consequences for oligodendrocyte-directed myelination (4, 11). Attractin's common biochemical role in immune cell interactions, regulation of pigmentation and neural pathology

remains undefined. A function in vesicular transport of cargo, both proteoglycan and new lipid-raft rich membrane, to the plasma membrane is implicated.

Methods:

Mice: Age-matched male C3HeB/FeJ mice and C3HeB/FeJ-*Atrn*$^{mg-3J/mg-3J}$ homozygotes were obtained from the Jackson Laboratory (Bar Harbor, ME). Animals were housed maximum 3 to a cage according to institutional guidelines in an Association for Assessment and Accreditation of Laboratory Animal Care (AAALAC)-accredited facility at the Dana-Farber Cancer Institute. Since Atrn mutations are recessive, homozygous *Atrn*$^{mg-3J/mg-3J}$ mice were mated with heterozygous *Atrn*$^{+/mg-3J}$ mice resulting in litters where half the mice were wild-type phenotype and half the mice were recessive *Atrn* mutants. In any experiment, only control and mutant siblings from the same mating were compared (aged 3–3.5 months), and comparisons examined mice with no gender preference. Euthanasia was by CO_2 inhalation followed by cervical dislocation with all procedures approved under Dana-Farber Cancer Institute Institutional Animal Care and Use Committee (IACUC) protocol 99 – 026.

Histology: Organs were excised and fixed in Bouin's fluid, formalin, or methanol depending upon the subsequent staining protocol. Tissues were then embedded in paraffin and 4 μm sections were arranged on glass slides. Hematoxylin and eosin staining followed standard histopathology procedures. For detection of glycoprotein, rehydrated sections were placed in periodic acid (0.5% in water) for 15 min, rinsed, placed in Schiff's reagent (0.5% in water; Sigma, St Louis MO), developed in running water and counterstained with hematoxylin prior to mounting. Photomicroscopic images were digitally captured using the "Magnafire" system (Olympus, Melville NY).

Results:

In this report we demonstrate that attractin-deficient *mahogany* mice, despite apparently normal gross organ structure, have a severe juvenile-onset progressive loss of basement membrane within organs heavily dependent upon extracellular matrix (ECM) function. Our attention was drawn to overall organ structure by the consistent observation that the spleens of older *Atrn*$^{mg-3J/mg-3J}$ mice (~ 5 months or more) are half to two-thirds the size of spleens from wild-type or heterozygous littermates (Fig. 1). Since the neuropathology in *Atrn*-null mice is moderate-to-severe at 2–4 months of age, we examined mice 3 to 3.5 months of age to determine if degeneration was occurring in tissues other than brain or spleen, including the kidney, liver and thymus. At this age, spleen size, cellularity and differential lymphocyte counts are comparable for wild-type and the *Atrn* mutants (data not presented). Kidney histology showed that the organization of individual nephrons seemed normal, but the interstitial matrix connecting the tubules was missing (Fig. 2A-D). Normal kidney stained well with Periodic Acid-Schiff (PAS) reagent but not with Alcian blue (data not presented) indicating that the normal interstitial matrix contains substantial levels of glycosylated protein including proteoglycan but little acid mucopolysaccharide. In contrast, kidney from *Atrn* mutants did not stain well with PAS indicating reduced extracellular

glycosylated material, particularly in the tubule brush border (Fig. 2E, F). Glycosylation of secreted proteins such as agouti destined for the extracellular compartment appears normal in *Atrn*$^{mg-3J/mg-3J}$ mice (5). Although a role for attractin in regulating specific glycosyltransferases cannot be excluded, the observed defects are consistent with a fault in extracellular matrix/proteoglycan secretion and deposition. In support, in the liver we find that the basement membrane between hepatocytes of wild-type mice is heavily stained but the ECM between the hepatocytes of *Atrn*$^{mg-3J/mg-3J}$ mice is strongly reduced. Further, the sinuses are swollen with reduced presence of the ECM-dependent space of Disse (Fig. 3C, D). Note the absence of glycogen in the mutant hepatocytes, probably consequent to the higher basal metabolic rate associated with the neurodegeneration-induced tremor (7). Using PAS staining, the liver of *Atrn*$^{mg-3J/mg-3J}$ also appears to be relatively deficient in glycosylated protein. In the thymus, where we believe attractin plays little role based on mRNA expression (1), there is no observable histological difference between control and mutant animals (data not shown).

Discussion:

We have been unable to demonstrate any interaction of either natural or recombinant attractin ectodomain with any component of the ECM, and attractin does not appear to be a component of the ECM. We propose that attractin functions in proteoglycan-rich granule exocytosis and ECM maintenance in the differentiated state, a process that will replenish the plasma membrane with new membrane as exocytosis occurs. Given its location in electron-dense granule-rich secretory vesicles (1), attractin may have evolved a secondary function for aiding transport to the exterior of positively charged peptides including agouti and certain chemokines. The reduction or absence of ECM-proteoglycan would have profound effects upon the presentation of basic peptides and chemokines that may account in part for the immune and pigmentation-related functionality of attractin (12, 13). The proposed role for vesicular trafficking attractin affecting ECM deposition and plasma membrane maintenance provides a unifying hypothesis for the pleiotropic effects of the null genotype and identifies avenues for further exploration. An additional consideration is that as yet unclassified human pathologies that involve neurodegeneration and concomitant renal dysfunction might be examined for abnormalities either at the *ATRN* locus or else its transcriptional control (14).

Limitations

Since these results describe pathology associated with a mutation in the *Atrn* gene, the only limitation concerns genetic penetrance. We have observed these results in the two most severe *Atrn* mutations (*Atrn*$^{mg-3J/mg-3J}$ and *Atrn*$^{mg-6J/mg-6J}$) but have not examined the *Atrn*$^{mg/mg}$ and *Atrn*$^{mg-L/mg-L}$ variants, strains with less severe effects upon levels of normal *Atrn* transcript (7).

Abbreviations:

α-MSH α-Melanocyte Stimulating Hormone

CNS: Central Nervous System

ECM: Extracellular Matrix

H&E: Haematoxylin and Eosin

IACUC: Institutional Animal Care and Use Committee

Mc1R: Melanocortin-1 Receptor

PAS: Periodic Acid-Schiff reagent

Declarations:

Ethics approval and consent to participate:

Animal studies were performed under Institutional Animal Care and Use Committee (IACUC)-approved protocol 99-026.

Consent for publication:

Not applicable.

Availability of data and materials:

All data generated or analysed during this study are included in this published article.

Competing interests:

The authors declare that they have no competing interests

Funding:

Not applicable.

Authors' contributions:

AA performed the experiments and pathology analysis. JSD-C directed the study and wrote the manuscript.

Acknowledgements:

Not applicable.

Authors' information (optional):

None.

References:

1. Duke-Cohan JS, Gu J, McLaughlin DF, Xu Y, Freeman GJ, Schlossman SF. Attractin (DPPT-L), a member of the CUB family of cell adhesion and guidance proteins, is secreted by activated human T lymphocytes and modulates immune cell interactions. Proc Natl Acad Sci U S A. 1998;95(19):11336–41.
2. Gunn TM, Miller KA, He L, Hyman RW, Davis RW, Azarani A, et al. The mouse mahogany locus encodes a transmembrane form of human attractin. Nature. 1999;398(6723):152–6.
3. Tang W, Gunn TM, McLaughlin DF, Barsh GS, Schlossman SF, Duke-Cohan JS. Secreted and membrane attractin result from alternative splicing of the human ATRN gene. Proc Natl Acad Sci U S A. 2000;97(11):6025–30.
4. Azouz A, Gunn TM, Duke-Cohan JS. Juvenile-onset loss of lipid-raft domains in attractin-deficient mice. Exp Cell Res. 2007;313(4):761–71.
5. He L, Gunn TM, Bouley DM, Lu XY, Watson SJ, Schlossman SF, et al. A biochemical function for attractin in agouti-induced pigmentation and obesity. Nat Genet. 2001;27(1):40–7.
6. Bronson RT, Donahue LR, Samples R, Kim JH, Naggert JK. Mice with mutations in the mahogany gene Atrn have cerebral spongiform changes. J Neuropathol Exp Neurol. 2001;60(7):724–30.
7. Gunn TM, Inui T, Kitada K, Ito S, Wakamatsu K, He L, et al. Molecular and phenotypic analysis of Attractin mutant mice. Genetics. 2001;158(4):1683–95.
8. Kuramoto T, Kitada K, Inui T, Sasaki Y, Ito K, Hase T, et al. Attractin/mahogany/zitter plays a critical role in myelination of the central nervous system. Proc Natl Acad Sci U S A. 2001;98(2):559–64.
9. Kuwamura M, Maeda M, Kuramoto T, Kitada K, Kanehara T, Moriyama M, et al. The myelin vacuolation (mv) rat with a null mutation in the attractin gene. Lab Invest. 2002;82(10):1279–86.
10. Kuramoto T, Nomoto T, Fujiwara A, Mizutani M, Sugimura T, Ushijima T. Insertional mutation of the Attractin gene in the black tremor hamster. Mamm Genome. 2002;13(1):36–40.
11. Tang W, Duke-Cohan JS. Human secreted attractin disrupts neurite formation in differentiating cortical neural cells in vitro. J Neuropathol Exp Neurol. 2002;61(9):767–77.
12. Vlodavsky I, Miao HQ, Medalion B, Danagher P, Ron D. Involvement of heparan sulfate and related molecules in sequestration and growth promoting activity of fibroblast growth factor. Cancer Metastasis Rev. 1996;15(2):177–86.
13. Billings PC, Pacifici M. Interactions of signaling proteins, growth factors and other proteins with heparan sulfate: mechanisms and mysteries. Connect Tissue Res. 2015;56(4):272–80.
14. Hirabayashi S, Shigematsu H, Iai M, Takashima S. A neurodegenerative disorder with early myoclonic encephalopathy, retinal pigmentary degeneration and nephronophthisis. Brain Dev. 2000;22(1):24–30.

1. Duke-Cohan JS, Gu J, McLaughlin DF, Xu Y, Freeman GJ, Schlossman SF. Attractin (DPPT-L), a member of the CUB family of cell adhesion and guidance proteins, is secreted by activated human T lymphocytes and modulates immune cell interactions. Proc Natl Acad Sci U S A. 1998;95(19):11336–41.
2. Gunn TM, Miller KA, He L, Hyman RW, Davis RW, Azarani A, et al. The mouse mahogany locus encodes a transmembrane form of human attractin. Nature. 1999;398(6723):152–6.
3. Tang W, Gunn TM, McLaughlin DF, Barsh GS, Schlossman SF, Duke-Cohan JS. Secreted and membrane attractin result from alternative splicing of the human ATRN gene. Proc Natl Acad Sci U S A. 2000;97(11):6025–30.
4. Azouz A, Gunn TM, Duke-Cohan JS. Juvenile-onset loss of lipid-raft domains in attractin-deficient mice. Exp Cell Res. 2007;313(4):761–71.
5. He L, Gunn TM, Bouley DM, Lu XY, Watson SJ, Schlossman SF, et al. A biochemical function for attractin in agouti-induced pigmentation and obesity. Nat Genet. 2001;27(1):40–7.
6. Bronson RT, Donahue LR, Samples R, Kim JH, Naggert JK. Mice with mutations in the mahogany gene Atrn have cerebral spongiform changes. J Neuropathol Exp Neurol. 2001;60(7):724–30.
7. Gunn TM, Inui T, Kitada K, Ito S, Wakamatsu K, He L, et al. Molecular and phenotypic analysis of Attractin mutant mice. Genetics. 2001;158(4):1683–95.
8. Kuramoto T, Kitada K, Inui T, Sasaki Y, Ito K, Hase T, et al. Attractin/mahogany/zitter plays a critical role in myelination of the central nervous system. Proc Natl Acad Sci U S A. 2001;98(2):559–64.
9. Kuwamura M, Maeda M, Kuramoto T, Kitada K, Kanehara T, Moriyama M, et al. The myelin vacuolation (mv) rat with a null mutation in the attractin gene. Lab Invest. 2002;82(10):1279–86.
10. Kuramoto T, Nomoto T, Fujiwara A, Mizutani M, Sugimura T, Ushijima T. Insertional mutation of the Attractin gene in the black tremor hamster. Mamm Genome. 2002;13(1):36–40.
11. Tang W, Duke-Cohan JS. Human secreted attractin disrupts neurite formation in differentiating cortical neural cells in vitro. J Neuropathol Exp Neurol. 2002;61(9):767–77.
12. Vlodavsky I, Miao HQ, Medalion B, Danagher P, Ron D. Involvement of heparan sulfate and related molecules in sequestration and growth promoting activity of fibroblast growth factor. Cancer Metastasis Rev. 1996;15(2):177–86.
13. Billings PC, Pacifici M. Interactions of signaling proteins, growth factors and other proteins with heparan sulfate: mechanisms and mysteries. Connect Tissue Res. 2015;56(4):272–80.
14. Hirabayashi S, Shigematsu H, Iai M, Takashima S. A neurodegenerative disorder with early myoclonic encephalopathy, retinal pigmentary degeneration and nephronophthisis. Brain Dev. 2000;22(1):24–30.

Figures

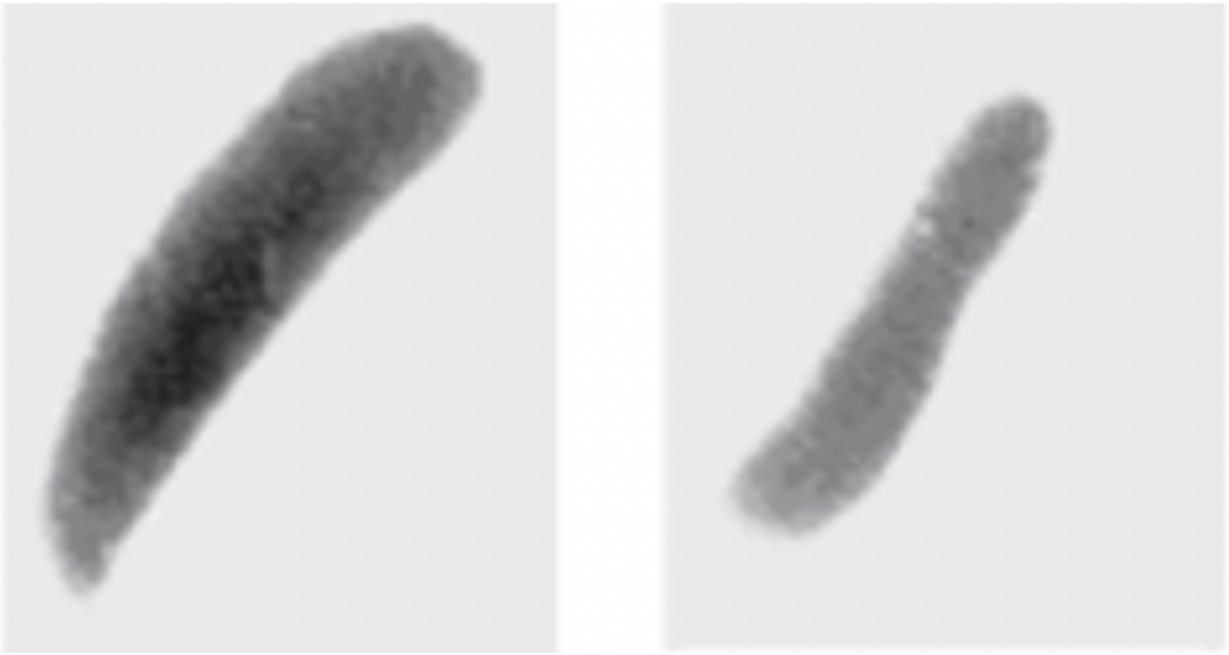

Figure 1

Spleens of older (~5 month) Atrnmg-3J/mg-3J mice (right panel; x3.5) are consistently half to two-thirds the size of age-matched controls (left panel; x3.5), reflected also by mononuclear cell counts (wild-type: 6.17 x 107 cells/spleen, Atrn-mutant: 3.9 x 107 cells/spleen; pool of 3 for each genotype).

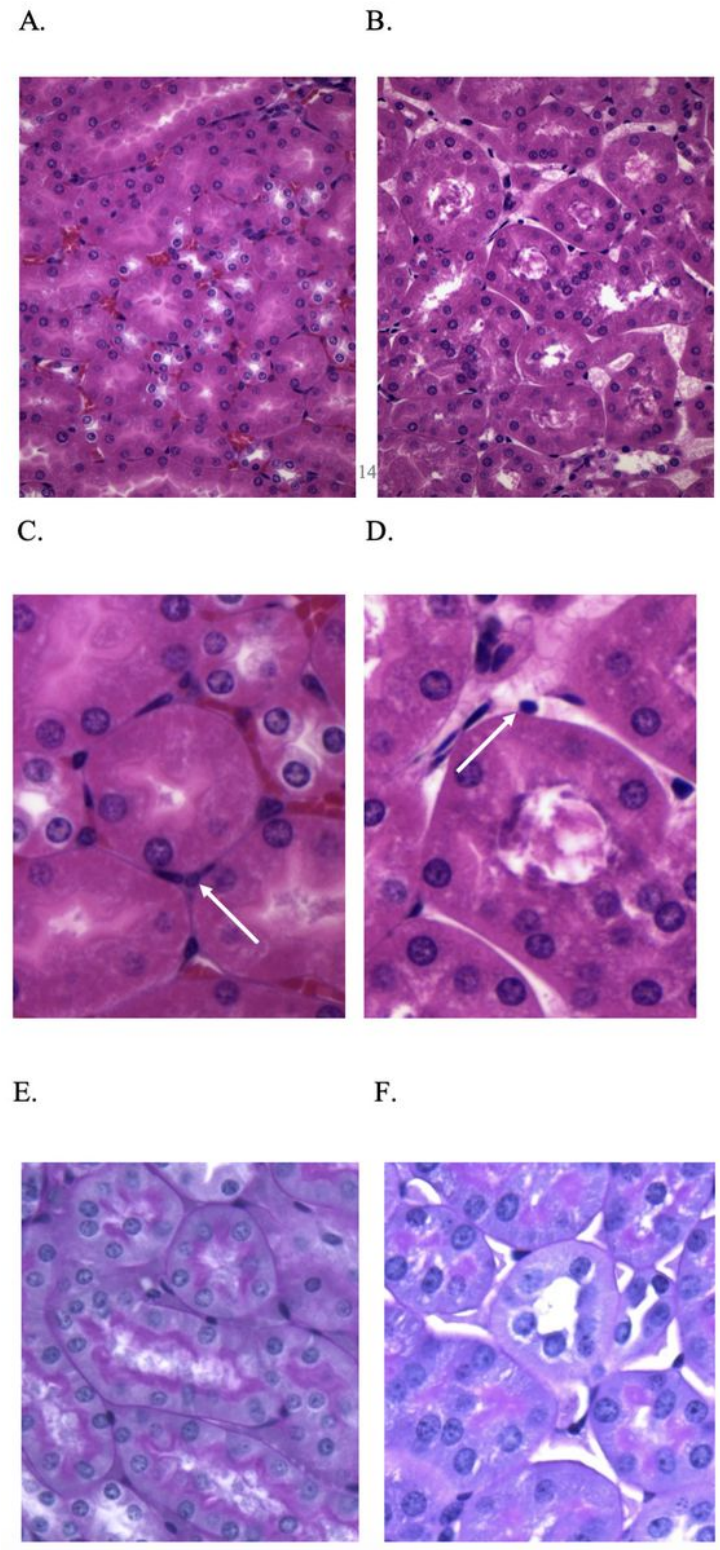

Figure 2

A. Normal kidney (H&E stain, x150); B. Atrnmg-3J/mg-3J kidney (H&E stain, x100). Note in the normal specimen the dense staining basement membrane surrounding each tubule which also forms a tight junction between the tubules. This staining is absent in the Atrn-mutant specimen. C. Normal kidney and D. Atrnmg-3J/mg-3J kidney (H&E stain, x300). In addition to the absence of intertubule ECM described in B, note that in both specimens there are interstitial cells between the tubules (arrows) but only in the

normal section are these cells embedded in basement membrane. E. Normal kidney and F. Atrnmg-3J/mg-3J kidney (PAS stain, x200). The brush border of Atrnmg-3J/mg-3J kidney is depleted of glycosylated protein on comparison with control, likewise for the intercellular space. For all images, results are representative of more than 5 sections from 10 paired sibling comparisons.

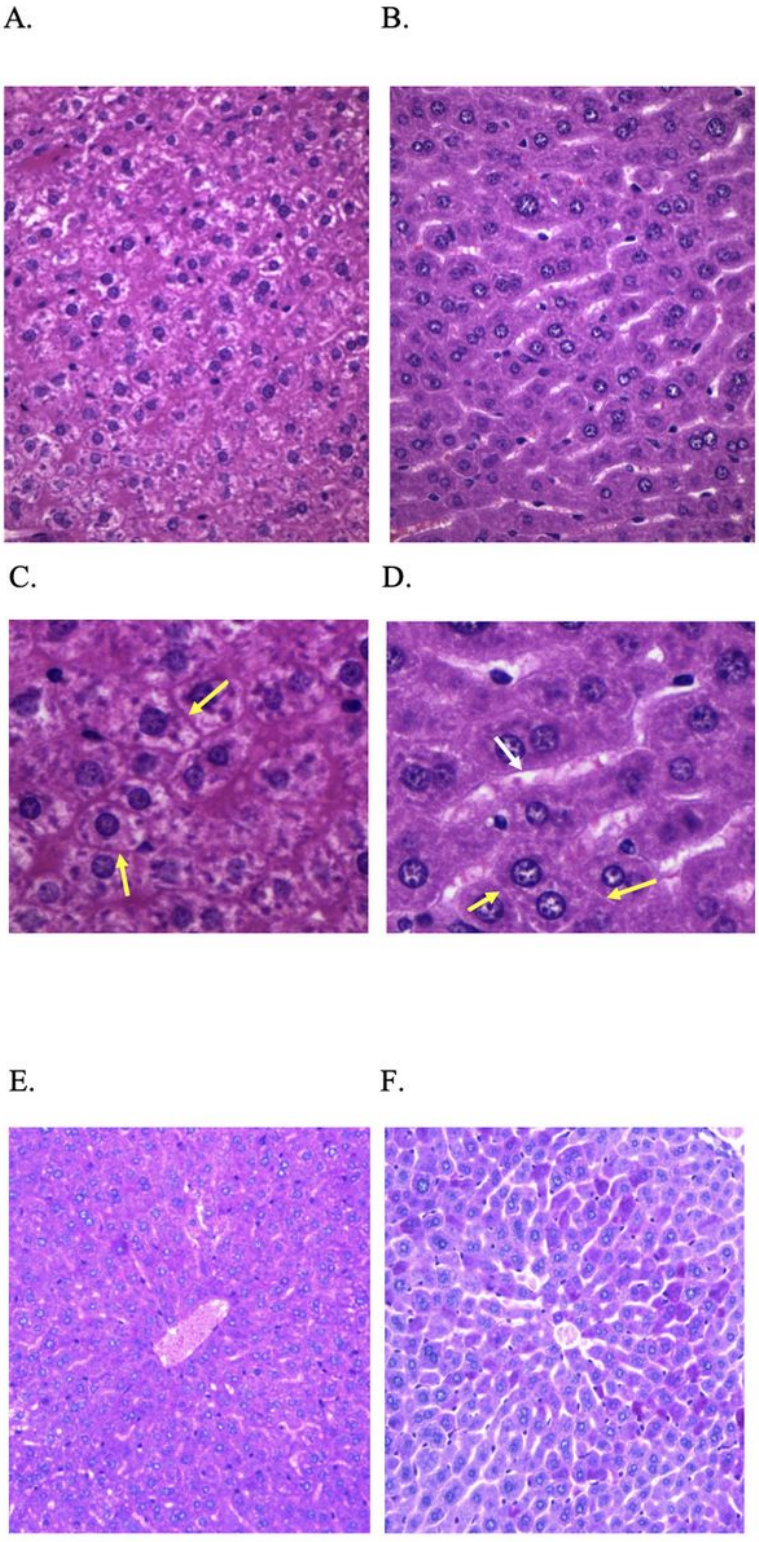

Figure 3

Normal liver and B. Atrnmg-3J/mg-3J liver (H&E stain, x100); The swollen sinuses are readily apparent in the mutant mice, as is the lack of dense staining of extracellular matrix between hepatocytes. Glycogen does not stain with H&E leading to white areas in the control cells, an effect not seen in the mutant indicating depletion of glycogen. C. Normal liver (H&E stain, x200; yellow arrows indicate space between hepatocytes). D. Atrnmg-3J/mg-3J liver (H&E stain, x200; white arrow identifies sinus, yellow arrows indicate space between hepatocytes). E. Normal liver and F. Atrnmg-3J/mg-3J liver (PAS stain, x50).

Supplementary Files

This is a list of supplementary files associated with this preprint. Click to download.

- NC3RsARRIVEChecklistAzouz2020BMCResNotesD.pdf